10 How Accretionary Prisms Elucidate Seismogenesis in Subduction Zones

J. Casey Moore, Christie Rowe, and Francesca Meneghini

Abstract

Earthquakes occur along the plate-boundary thrusts underlying accretionary prisms and along out-of-sequence thrusts that cut through prisms. Thermal models suggest that the earthquakes on the plate-boundary thrusts initiate in a temperature range of 125ºC to ~350ºC. Because syndeformational diagenetic and metamorphic alterations recorded in accretionary prisms have specific temperature ranges, the alterations and the associated deformation can be correlated to the temperature range that accretionary prisms are seismogenic. Comparison of accreted rocks deformed above, within, and below the seismogenic zone suggests characteristics of rocks at seismogenic depths that may make them earthquake prone. During passage through temperatures from 50º to 150ºC, accretionary prism sediments become rocks, undergoing diagenetic reactions including the transformation of smectite to illite, albitization of detrital feldspar, dehydration of opal, and the generation of hydrocarbons. Although the smectite to illite transition does not change the frictional properties of the prism so that it becomes seismogenic, water and cations (calcium, magnesium, iron) released during this transition and the albitization process foster cementation. Cementation and veining by carbonates becomes common by 125ºC, perhaps due to the above-mentioned release of cations. Pressure-solution fabrics begin to be apparent at ~150ºC, with well-developed cleavages and quartz veining common by 200ºC. Pressure solution may be facilitated by the diagenetic formation of illite. Quartz veining and cementation in the 150º–300ºC range facilitates the change from a velocity-strengthening, clay-dominated to a velocity-weakening, quartz-influenced, earthquake-prone rheology. The diagenetic-metamorphic reactions occurring at temperatures from 125º to ~300ºC cement and add rigidity to the thickening upper plate of the accretionary prism. This developing elastic strength of the upper plate is

required to store the elastic strain energy required for an earthquake. In accretionary prisms, brittle fabrics are progressively replaced by ductile fabrics through a temperature range of ~150°–325°C. Although rocks in the seismogenic zone have lost most of their intergranular fluid through consolidation, vein geometries and fluid inclusions suggest high fluid pressures, approaching lithostatic. Strain localization in the form of discrete shear surfaces occurs across the lower aseismic to seismic transition. Strain localization is observed both at outcrop and map scale. At map scale, the seawardmost occurrence of out-of-sequence thrusts defines the leading edge of the rigidified accretionary prism that is capable of storing elastic energy.

Introduction

Accretionary prisms comprise materials that have been transferred from the oceanic plate to the overriding plate in subduction zones. At all but the shallowest levels, near the front of the prism, these sediments and rocks have been underthrust with the lower plate and accreted to the upper plate (fig. 10.1). This accretion process involves a downward migration of the subduction thrust. Thus accretionary prisms constructed by this "underplating" process include faults that were for a period of time subduction thrusts. In addition to the faults active during the initial emplacement of their rocks, accretionary prisms are cut by later faults, or out-of-sequence thrusts. In combination, the basal subduction thrusts and the later faults encompass faults active in the great subduction earthquakes [*Plafker*, 1972], the largest known seismic

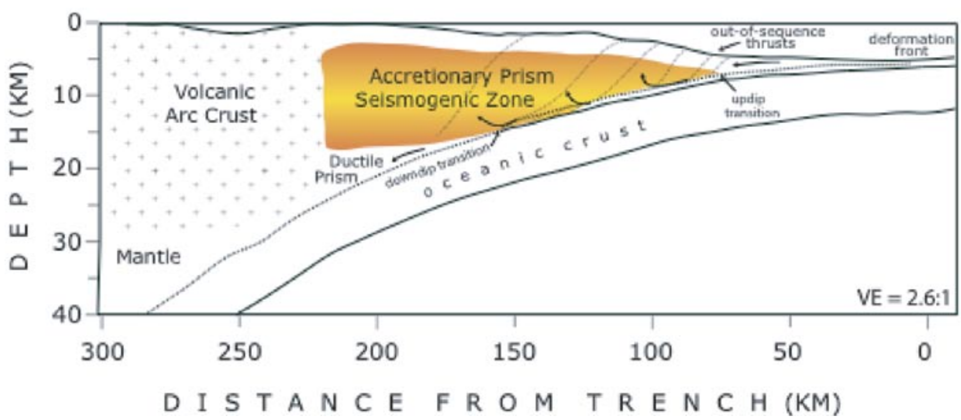

Figure 10.1 Cross section showing transport paths of rocks through the accretionary prism. Note that out-of-sequence thrusts begin at about seaward limit of prism seismogenic zone. Seismogenic zone defined by temperature limits of 125°–350°C; limits would shift with variations in geothermal gradient. Arrows show material transport paths in prism.

events [*Lay and Bilek*, this volume). The history of deformation through the earthquake cycle is recorded in the rocks of accretionary prisms. To the degree that we can decipher this history, we can learn much about the inception and evolution of the deformational processes associated with earthquakes.

Investigation of old rocks from the seismogenic realm provides windows on processes that cannot be observed short of deep drilling. Terranes of old rocks allow direct investigation of three-dimensional variations, which will be useful in interpreting any results from more physically limited boreholes. However, investigations of old rocks are constrained in that they offer an interpretable record of past activity but do not allow direct observation of active processes.

Defining the Seismogenic Zone at Convergent Plate Boundaries

The seismogenic zone is most properly defined by a depth interval of unstable (stick-slip) frictional behavior where earthquakes can initiate [*Scholz*, 2002, p. 152]. In practice, this depth interval can best be identified by aftershock zones of large earthquakes. In the absence of well-resolved aftershock distributions, coseismic rupture areas estimated from earthquake and/or tsunami wave inversions have been used to infer the limits of the seismogenic zone. Because coseismic rupture may propagate into a zone of conditional stability or even marginally into the unstable regime [*Scholz*, 2002, p. 88], coseismic rupture may overestimate the seismogenic zone as defined above. Geodetic measurements indicating the distribution of locking or partial locking can define the seismogenic zone [*Norabuena et al.*, 2004]. Interseismic microearthquakes have been used to estimate the limits of the seismogenic zone [e.g., *Obana et al.*, 2003] but may only be active over part of the seismogenic zone of large earthquakes [*Schwartz and Deshon*, this volume]. In summary, aftershock distribution and locked intervals inferred from geodetic measurements probably provide the best practical means of locating the seismogenic zone.

Recognizing Faults Rocks from the Seismogenic Zone

Progressive addition or underplating of material at the base of accretionary prisms results in their uplift. Therefore the oldest rocks, exhumed from the deepest level, are the structurally highest, and commonly innermost parts of the continually accreted prism, with less deeply buried rocks progressively exposed in a seaward direction [*Brandon and Vance*, 1992; *Plafker et al.*, 1994; *Taira et al.*, 1988]. Typically, packages of rocks with internally similar sedimentary, deformational, and metamorphic histories are separated from each other by prominent out-of-sequence thrust faults. The best-exposed packages of ancient accreted rocks occur where subduction was characterized by a generally high input of sediment and consequent creation and uplift of a volumetrically significant accretionary prism, for example, prisms in California, Washington, Alaska, and southwestern Japan. Even though these accretionary prisms are dominated by clastic rocks of the high sediment input intervals, selected sections include units formed during periods of low sediment supply, in which the subduction zone was more sediment starved. Therefore studies of these ancient rocks can provide information on seismogenesis in both sediment-dominated and sediment-poor systems.

Given exhumed prism rocks of a range of ages, metamorphic grades, and structural styles, how can we recognize rocks that have deformed at the seismogenic zone? Pseudotachylytes, or rocks formed by frictional melting on fault surfaces, are most explicit evidence of past seismogenic behavior [*Cowan*, 1999; *Sibson*, 1975]. However, pseudotachylytes are rare in accretionary prisms [*Ikesawa et al.*, 2003], and there is much disagreement on what structural features may actually form during a seismic event [e.g. *Cowan*, 1999]. A more inclusive approach to understanding rocks that have behaved seismogenically is to simply investigate faults in any volume of rock that has deformed through the P-T conditions where modern earthquakes occur. We can reasonably infer that these rocks have in part deformed seismogenically and that this deformation occurred along brittle structural features. Thus we are asking not whether a particular structure represents a seismogenic, or high-velocity, displacement [see *Cowan*, 1999] but what features of rocks in the seismogenic zone may lead to stick-slip behavior. Accordingly, comparison of these rocks to those that behaved aseismically at shallower and greater depths provides insights on the rock fabrics and material properties that control seismogenic behavior.

During the last decade, thermal models [*Currie et al.*, 2002; *Hyndman et al.*, 1997; *Oleskevich et al.*, 1999; *Wang*, 1995] have defined the temperature range at which modern interplate earthquakes occur at seismogenic zones. The temperature range of large interplate thrust earthquakes is from 100º–150ºC to 350º–450ºC, with the depth limits varying depending on the thermal gradient of the associated subduction zone. The extreme deeper limit of the seismogenic zone may be due to earthquakes initiating at temperatures <350ºC but propagating in to a conditionally stable region at temperatures perhaps as high as 450ºC. Although there are undoubtedly significant errors in the thermal models, the consistency of temperature ranges for interplate thrust earthquakes at modern subduction zones provides confidence that the above-mentioned temperature limits for the seismogenic zone can be used to define the temperature limits of seismogenic activity in ancient rocks (figs. 10.2 and 10.3). For example, it may be difficult to identify exact temperatures of the boundaries, we can be confident at 50ºC we have not reached the seismogenic zone, at 200º–300ºC we are within the seismogenic zone, and at 450ºC we are beyond the seismogenic zone.

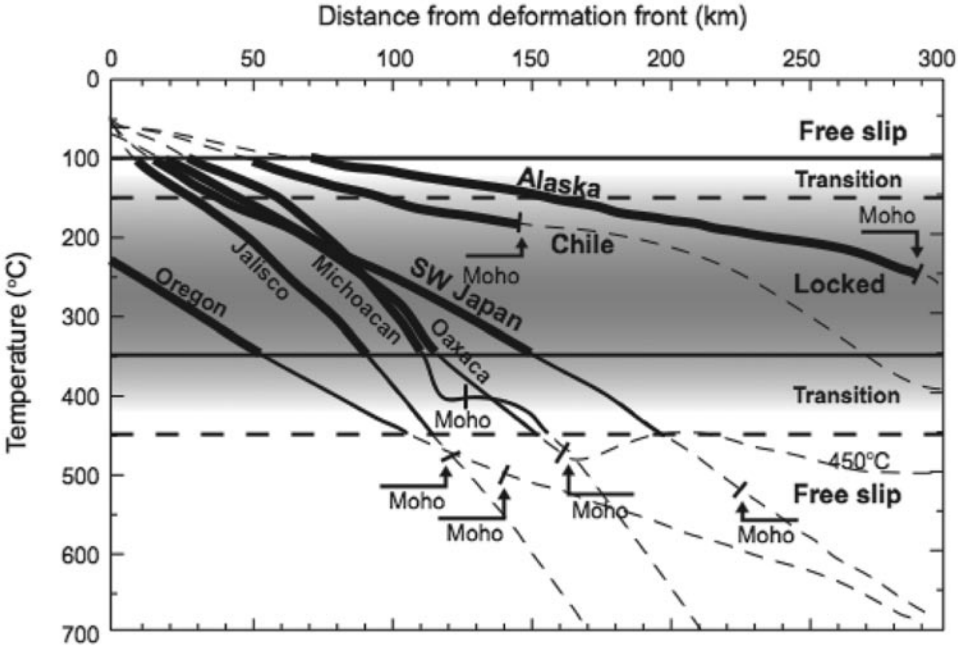

Figure 10.2 Compilation of modeled temperatures of subduction thrust interfaces verses distance landward of deformation front. Temperatures estimated from two-dimensional thermal models with upper and lower bounds of seismogenic zone estimated from aftershocks or modeled fault slip from seismic and/or tsunami waves [*Currie et al.*, 2002; *Hyndman*, 1997]. Note the transitional nature of both the upper and lower boundaries to the locked seismogenic zone.

Pinpointing fault rock units deforming in the seismogenic temperature range requires identification of syndeformational metamorphic minerals [*Ernst*, 1990], or the use of fluid inclusion P-T estimates derived from syndeformational minerals [*Vrolijk et al.*, 1988] that formed under seismogenic P-T conditions (fig. 10.3). Plotting the P-T limits of the seismogenic zone on a petrogenetic grid then ties the seismogenic zone to observable minerals formed syntectonically (fig. 10.3). We have used 350°C as the higher-temperature cutoff of the seismogenic zone overlain on the petrogenetic grid. By that temperature, quartz is ductile and most accreted sediments are highly siliceous, so we expect aseismic behavior above 350°C.

Within rock units deformed at seismogenic depths, we can recognize ductile deformation that would be occurring during interseismic intervals. We can also identify brittle failure surfaces of high strain that may or may not represent deformation at seismogenic strain rates [*Cowan*, 1999]. We agree that unambiguous identification of seismic slip surfaces, except pseudotachylyte, is ambiguous. However, we are studying rocks deformed in the accretionary prism realm that have suffered the effects of the largest earthquakes in the

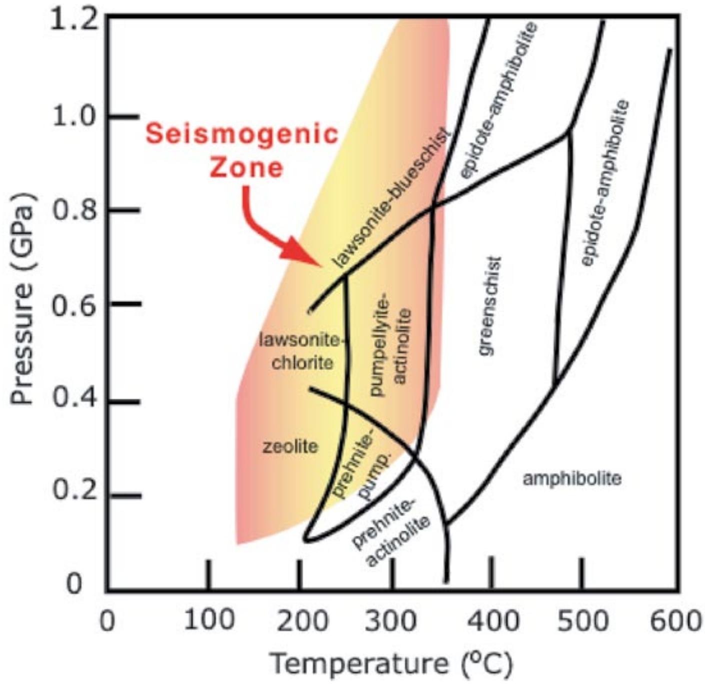

Figure 10.3 P-T limits of seismogenic zone estimated from modeled temperature limits of modern systems (125°–350°C) limited by thermal gradients from ancient prisms. Upper pressure limit constrained by extremely cold subduction systems such as ancient Franciscan Complex [*Ernst*, 1990] and lower limits by very warm systems such as the Shimanto Complex of southwestern Japan [*Lewis and Byrne*, 2003] and Cascadia subduction zone [*Hyndman and Wang*, 1993]. Limits of metamorphic mineral facies from *Peacock* [1993].

world. Thus it is statistically likely that some of the brittle failure surfaces in these rocks record coseimic slip. This must be particularly true at subduction zones similar to the Cascadia margin where nearly 100% of interplate motion must be accommodated coseismically at the depths the seismogenic zone is completely locked [*Wang et al.*, 2003].

Distribution of Deformation in the Seismogenic Zone

As depicted in figure 10.2, the seismogenic zone comprises a rock volume, not just a two-dimensional interface along the basal subduction thrust. Although major slip on large earthquakes is concentrated on the basal thrust and out-of-sequence thrusts [*Plafker*, 1972], small earthquakes occur through the seismogenic portion of the accretionary prism [*Lewis et al.*, 2003]. Structural studies suggest that the major deformation of the prism rocks occurs along the subduction thrust. Structural analyses indicate that accretionary prism deformational fabrics are largely acquired during the initial emplacement of the rocks [*Fisher and Byrne*, 1987; *Kusky and Bradley*, 1999], However, faulting [e.g., *Lewis and Byrne*, 2003] and interseismic ductile deformation [e.g., *Fisher and Byrne*, 1992] continue in the seismogenic interior of the accretionary prism. The sequence of structural superpositions is normally clear. Our summary attempts to encompass all the mineralogical changes and structural fabrics developed in the seismogenic zone of the accretionary prism, whether along the high-strain basal region, on out-of-sequence thrusts, or in lower-strain rate interior regions.

What Progressive Changes Occur in Mineralogy and Fault Rock Fabrics Into and Through the Seismogenic Zone?

Our discussion is based on cataloging and organizing the mineralogical and microscopic to outcrop-scale deformational features observed in accretionary prism rocks that have been deformed at P-T conditions above, within, and below the seismogenic zone (table 10.1). Although related, evidence for fluids, fluid pressure, and strain localization are discussed separately. Metamorphic and deformational phenomena tabulated in figure 10.4 illustrate the broad trends from the upper aseismic zone through the seismogenic zone into the lower aseismic zone. Although the boundaries between these realms are transitional, major changes are apparent from one to another.

As used in this paper and in figure 10.4, "brittle deformation" is associated with loss of cohesion along fractures and faults, and "ductile deformation" refers to coherent nonrecoverable deformation without fracturing at scale of crystal grains or larger [*Twiss and Moores*, 1992; *van der Pluijm and Marshak*, 1997, 2004]. Following these authors, we include cataclasis and granular flow in brittle deformation because cataclasis involves brittle fracture and they are both controlled by frictional rheology. Optical microscopic investigations clearly distinguish brittle and ductile phenomena, as defined above, and these observations can be extended to hand specimen and outcrop scales to distinguish brittle and ductile fabrics.

Observations

Diagenesis to Low-Grade Metamorphism Our discussion of metamorphic mineral transitions occurring in subducted rocks [e.g., *Ernst*, 1990] only focuses on a few alterations that apparently strongly influence the structural

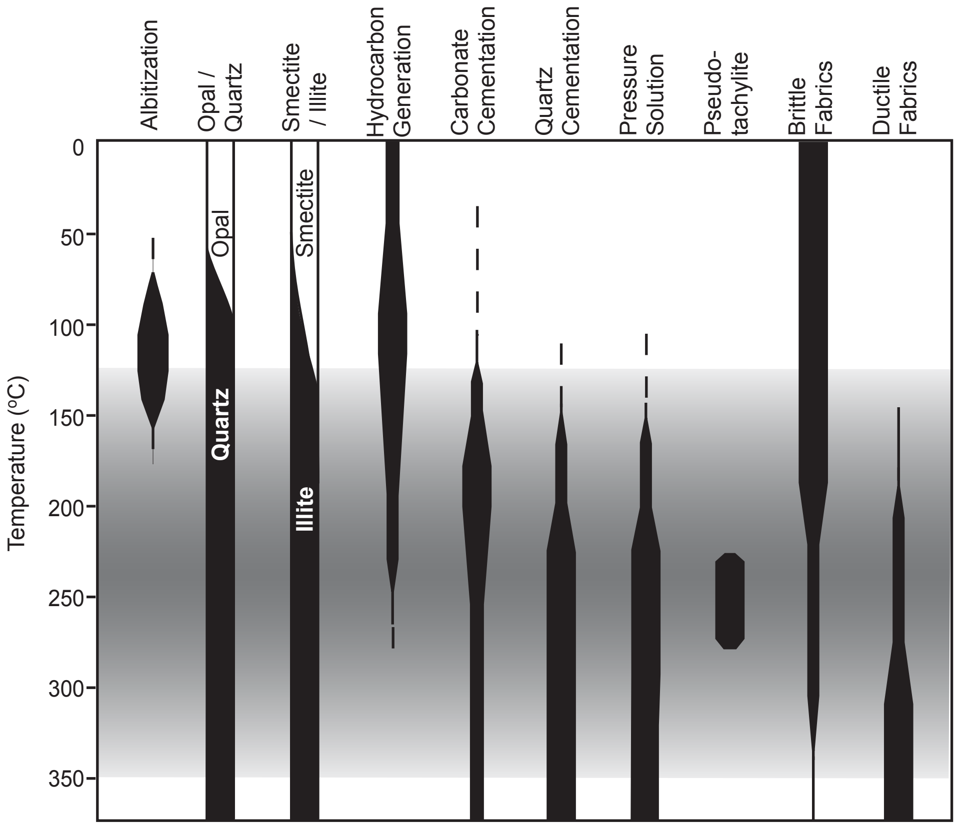

Figure 10.4 Mineralogical transitions and fabric changes in the 0°–375°C temperature range in accretionary prism. Abundance of minerals as well as intensity of metamorphic and structural processes is shown schematically by width of bars. Temperature range of pseudotachylyte (frictional melt) is that of country rocks in which melting occurred. Information on this diagram is generalized from sources in table 10.1 and references cited in discussion section.

evolution of the rocks. Of these, the formation of metamorphic albite releases calcium from more calcic-rich detrital plagioclase [*Boles*, 1982]. The transition from smectite to illite releases water, calcium, iron, and magnesium [*Boles and Franks*, 1979]. Sediments incoming to the subduction zone may include biogenic opal (diatoms or radiolarians) or opal in volcanic glass. Both transform to quartz below 100ºC, causing a decrease in solid volume, and water production [*Behl and Garrison*, 1994; *Isaacs et al.*, 1983]. Hydrocarbon production begins near the surface peaks around 100ºC and declines with the production of methane to above 200ºC [*Hunt*, 1996]. Hydrocarbon production not only provides fluid by various carbon species that can influence mineral precipitation but also low density fluids that can lead to overpressuring.

TABLE 10.1 **Observed Cements, Veins, and Relevant Structural Fabrics in Various Temperature and Metamorphic Facies Ranges**

Temperature and Pressure Range	Observations and Source Localities	References
<100ºC Unmetamorphosed	No veins and cements through nearly all cored rocks in ODP. Minor carbonates in Barbados drill cores. Extremely rare quartz, carbonate, and sulfides in Nankai Trough. Accreted terrigenous deposits on Barbados Island lack any carbonate/quartz veins or cements. Faulting and stratal disruption includes cataclasis of sand sized particles widespread development of scaly fabric in mudstones.	*Byrne et al.*, 1993; *Labaume et al.*, 1997; *Maltman et al.*, 1993, 1997; *Moore and Allwardt*, 1980; *Speed*, 1990; *Vrolijk and Sheppard*, 1991.
100º–150ºC; 5 km Typically Zeolite Facies	Evidence for cementation and veining variable. Locally significant carbonate cementation along fault zones. Quartz cementation/veins rare and minor. Cataclasis of sand-sized particles widespread. Development of scaly fabric in mudstones. Incipient pressure solution cleavage.	*Geddes*, 1993; *Moore*, 1980; *Moore and Allwardt*, 1980; *Orange et al.*, 1993; *Orange and Underwood*, 1995; *Rowe et al.*, 2002.
150º–300ºC; 5–15 km Typically Prehnite-Pumpellyite Facies	Quartz- and carbonate-veining common. Cataclasis in sands and veined materials temporally alternates with pressure solution. Cleavages common, and especially visible in more coherent units. Quartz veins/cements common in the 200º–300ºC range. Rare pseudotachylyte.	*Byrne*, 1984; *DiTullio and Byrne*, 1990; *DiTullio et al.*, 1993; *Fisher*, 1996; *Hibbard et al.*, 1993; *Ikesawa et al.*, 2003; *Kimura and Mukai*, 1990; *Onishi and Kimura*, 1995; *Sample and Moore*, 1987; *Sample*, 1990; *Vrolijk et al.*, 1988.
150º–350ºC; 15–27 km Classic HP-LT (e.g., Franciscan Blueschists of eastern belt)	Often coherent layering with multiple fold generations, local stratal disruption predating metamorphism. Pressure solution common.	*Jayko et al.*, 1986; *Ring and Brandon*, 1999.
>300ºC; 8-27 km Prehnite-Actinolite, and Blueschist-Greenschist Facies	Widespread foliation development, pressure solution, microscopically apparent recrystallization during development of metamorphic assemblages. Many terranes surprising coherent with multiple phases of folding. Brittle deformation during peak metamorphism not obvious, but a previous history is suggested by the stratal disruption in some areas.	*Helper*, 1986; *Norris and Bishop*, 1990; *Ring and Brandon*, 1999; *Roeske*, 1986; *Schwartz and Stockhert*, 1996.

[a] Temperature ranges are associated with typical metamorphic facies with actual temperature conditions determined from metamorphic minerals, fluid inclusions, and vitrinite reflectance. The pressure and temperature range encompass those of the cited examples with the associated metamorphic facies being identified. The P-T ranges do not include the maximum range of the particular metamorphic facies. Surface and near-surface carbonate precipitates associated with cold seeps not included as their formation is too shallow to be involved in seismicity.

Cements and Veins We focus on veins and cements that can be observed petrographically, excluding subtle clay cements that may be easily obscured by mechanical deformation. Observations from Ocean Drilling Program/Deep Sea Drilling Project (ODP/DSDP) cores and the few exposures of shallowly buried accretionary prisms indicate that they are generally uncemented and sparsely veined below 125°C, excluding carbonates formed by surface seepage [*Kulm and Suess,* 1990] and are not involved in seismogenesis. Above these temperatures, calcite is locally abundant to the 150°–250°C range. Quartz veining is not common until ~200°C. In prism rocks exposed on land, veins and cements occur both distributed through the rocks (fig. 10.5) and in locally high concentrations in fault zones (fig. 10.6). The distributed veins occur in extensional fractures in boudins or in fractures in coherent rock units and also coat shear surfaces of boudins and distributed faults. The extensional veins inside the boudins are protected from the destructive slip processes occurring along shear surfaces coating boudins, perhaps accounting for their abundance over shear veins at some localities.

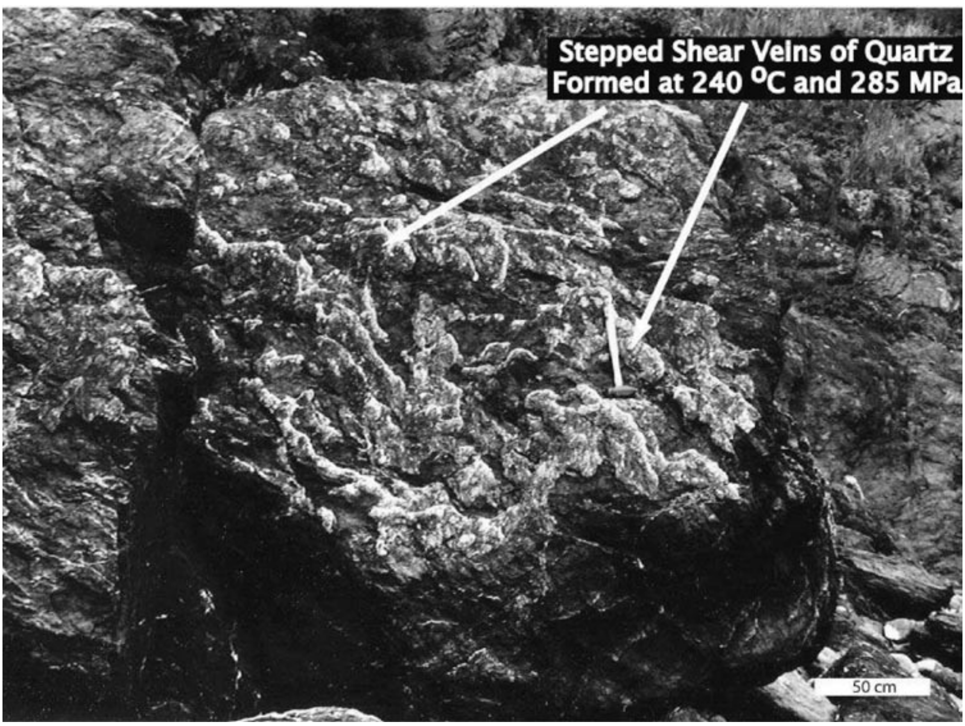

Figure 10.5 Photograph of quartz-veined block surface of stratally disrupted zone, Paleocene accretionary prism, Kodiak Islands, Alaska [*Vrolijk et al.*, 1988]. Shear veins coating surface of this block probably developed during interseismic phase of deformation but would provide a quartz-influenced rheology during seismic deformation.

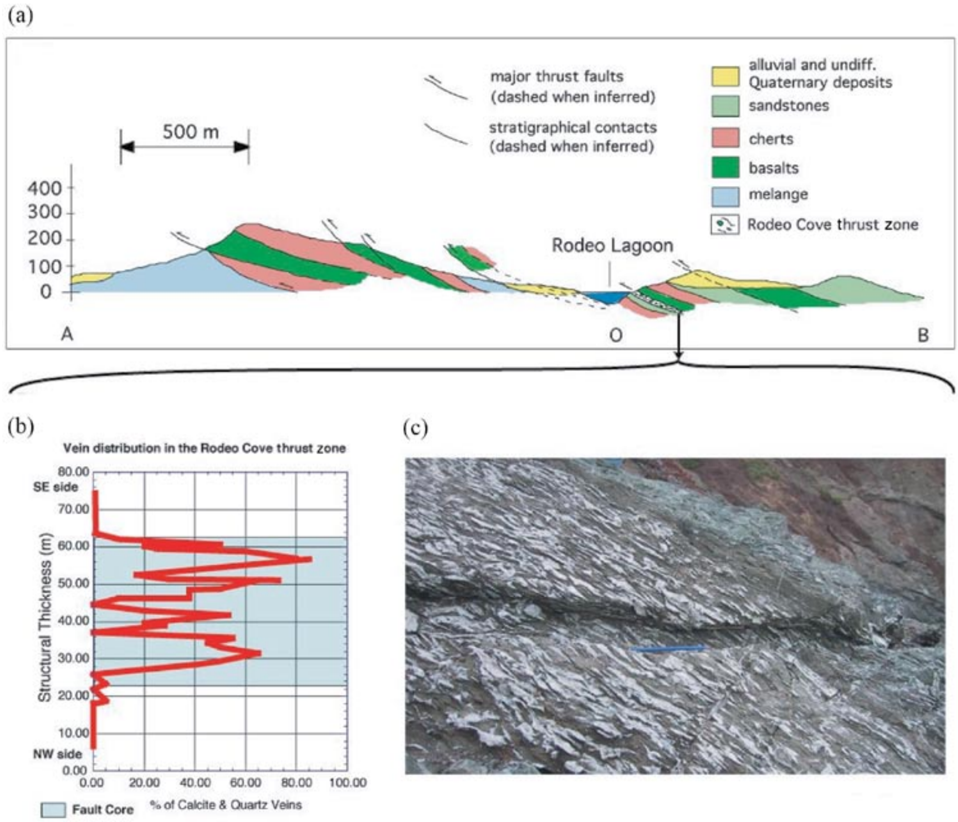

Figure 10.6 Evidence for localized fluid flow on a subduction thrust system. (a) Cross section viewed to the ENE through Rodeo Cove area, Marin Headlands [*Blake et al.*, 2000]. (b) Concentration of carbonate and quartz veins in Rodeo Cove thrust zone [*Meneghini*, 2003]. Percentage of veins reflects average over decimeter intervals. (c) Outcrop of carbonate and quartz veins in Rodeo Cove thrust zone. Note parallelism of veins to dip of fault zone in fig. 10.6a. Veins are also parallel to pressure-solution foliation in fault zone [*Meneghini*, 2003]

Brittle Deformation Brittle deformation includes fabrics associated with faulting in subduction zones: scaly fabric (mudstone), stratal disruption, and the associated development of complex cataclastic shear bands as well as macroscopically discrete shear surfaces [*Moore*, 1986]. In subduction zones, cataclastic phenomena are commonly localized into millimeter-wide shear bands [*Aydin*, 1978] of complex three-dimensional geometry, or "web structure" [*Byrne*, 1984]. Apparently, the shear bands achieve their complex three-dimensional structure because of the ongoing rotational deformation and high strain that ultimately result in stratal disruption. Granular flow and distributed cataclastic flow occur at the earliest phases of development of subduction shear zones [*Lucas and Moore*, 1986]. Pseudotachylyte is rare and developed in rocks with background temperatures of 230º–270°C prior to melting at much higher temperatures [*Ikesawa et al.,* 2003; *Kitamura et al.,* 2005; *Rowe et al.*, 2005].

Ductile Deformation Pressure solution is the initial ductile deformation mechanism in accretionary prisms. At temperatures <140º–150°C pressure solution is subtle, characterized by local indentation and suturing of grains. At higher temperatures, solution processes begin to produce cleavages of increasing intensity. Pressure solution is the most dominant ductile deformation mechanism in accretionary prisms [*Feehan and Brandon,* 1999; *Fisher and Byrne,* 1992; *Fisher and Brantley,* 1993; *Ring and Brandon,* 1999; *Schwartz and Stockhert,* 1996]. Because pressure solution is commonly superimposed on previously stratally disrupted units, strong planar cleavages are not always obvious. Pressure solution apparently remains the dominant ductile deformation mechanism to temperatures exceeding 350°C. Intracrystalline deformation along dislocations is relatively rare [*Schwartz and Stockhert,* 1996], but the rocks undergo syntectonic recrystallization during growth of new phases, for example [*Jayko et al.,* 1986].

Discussion

Above we subdivide the critical diagenetic-metamorphic and deformational processes operating in both aseismic and seismic realms of accretionary prisms. Linkages exist between many of these processes and together control deformation and earthquake generation in this environment. Below we provide some interpretations on how these processes are interrelated and foster seismogenesis.

Smectite-Illite Transition and Albitization The smectite to illite transition, which is virtually complete at 150ºC, was proposed as a possible cause of the upper aseismic to seismic transition in subduction zones (fig. 10.1) [*Hyndman,* 1997; *Vrolijk,* 1990] because this phase transition causes an increase in coefficient of friction (or strengthening of fault surfaces). However, recent experimental work on the rate-dependent frictional properties of illite shows that it is velocity strengthening [*Morrow et al.,* 1992; *Saffer and Marone,* 2003], which is not consistent with accelerating runaway slip behavior associated with an earthquake [*Scholz,* 2002].

Although the smectite to illite transition may not have a direct physical effect on seismogenesis, the chemistry of the phase change may be significant. The smectite to illite transition produces calcium, iron, and magnesium, which are expelled into pore waters. The albitization of plagioclase also produces calcium over about the same temperature range as the smectite to illite transition. The influx of these cations is thought to cause carbonate cementation during burial of sedimentary rocks [*Boles and Franks*, 1979] and also in accretionary prisms [*Sample*, 1990].

Carbonate Cementation Carbonate cementation/veining occurs in significant amounts starting at ~100º–150ºC, which may reflect an influx of calcium, iron, and magnesium causing the concentrations of these cations in pore waters to exceed the solubility of the various carbonate minerals. CO_3^{-2} in the carbonates is probably ultimately derived from organic matter [*Mullis et al.*, 1994], especially because limestones are rare in accretionary prisms. The presence of interstitial carbonate can add to the cohesion of the rock volume and perhaps change its response to deformation [*Muhuri et al.*, 2003]. It is not clear whether carbonate is velocity weakening or velocity strengthening [*Lockner and Byerlee*, 1986], and therefore its significance in modifying the frictional response of discrete fault zones is underdetermined. Carbonate cementation is one process that would rigidify the accretionary prism and therefore contribute to its elastic strength and earthquake potential (see below). Carbonate cementation would also reduce porosity and permeability and foster high fluid pressure.

Pressure Solution and Quartz Cementation Pressure solution is normally considered as a component of diffusive mass transfer (dissolution, diffusion, and precipitation). Because fluid advection and diffusion are both important in the transport of solutes in accretionary prisms, we focus our discussion on the dissolution and reprecipitation of materials. The onset of pressure solution appears approximately when the smectite to illite transition is complete. Research by sedimentary petrologists indicates that dissolution is strongly is facilitated by the presence of an illite-muscovite phase under very low stresses [*Bjorkum*, 1996]. Therefore the combination of increasing temperature, increasing effective stress, and the increase in abundance of illite from the smectite-illite transition may cause the onset of pressure solution observed at ~150ºC in accretionary prisms. This interpretation suggests additional importance of the smectite-illite transition as a chemical, if not a physical, transition increasing rock coherence and possibly contributing to seismogenic potential.

Byrne [1998] has suggested diffusive mass-transfer processes homogenize rock fabrics and therefore allow generation of recordable earthquakes. *Rowe and Moore* [2003] further pointed out that the common quartz veining and cements occurring in areas of pressure solution change the frictional properties of the rock, leading to a velocity-weakening slip behavior. Apparently, silica is being mobilized by dissolution and redeposited at temperatures >150ºC, well within the 100º–300ºC temperature range where quartz demonstrates velocity-weakening behavior [*Blanpied et al.*, 1995] (fig. 10.7). Other experiments suggest quartz is velocity weakening even at lower temperatures [*Di Toro et al.*, 2004]. However, faults in accretionary prisms are clay dominated at lower temperatures, so the onset of quartz deposition in faults above 150ºC is an important control on their stick-slip behavior.

Schwartz and Stockhert [1996] argued that the abundance of pressure solution and paucity of intracrystalline deformation is due to the low stresses in accretionary prisms, relative to continental deformation. Because accretionary prisms are thrust systems, higher mean stresses might be expected for a given

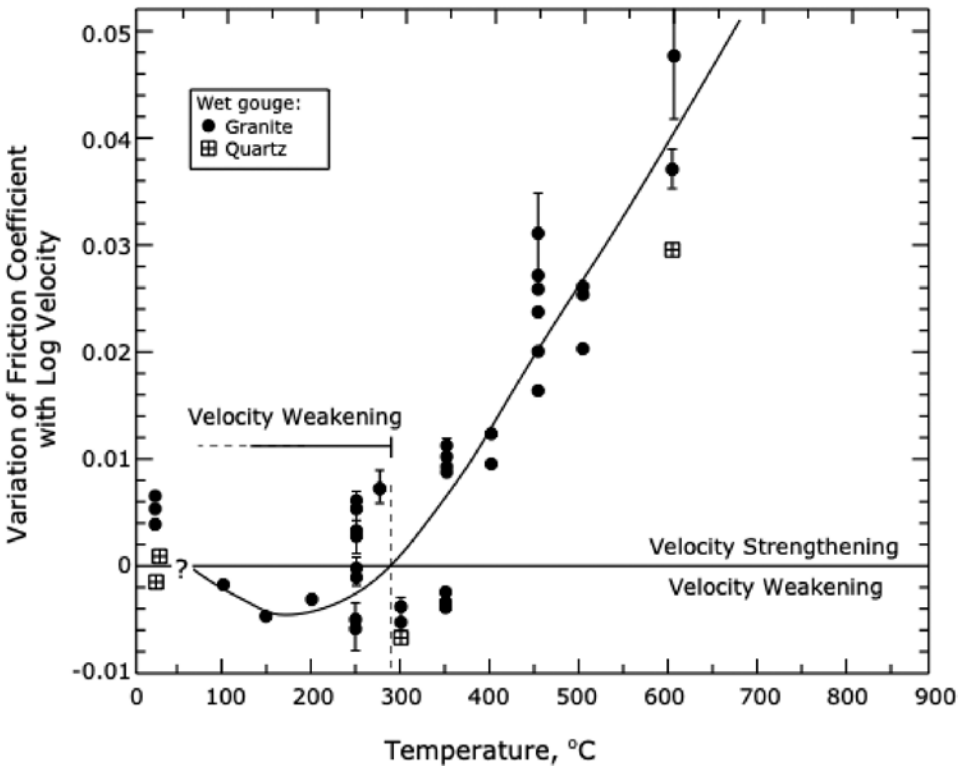

Figure 10.7 Velocity dependence of granite and quartz gouge samples [*Blanpied et al.*, 1995]. Note that velocity weakening occurs below ~300°C. The lower limit of velocity weakening is poorly determined. However, fault zones in accretionary prisms are clay dominated below ~150°C, which would favor stable sliding. The infusion of quartz into faults above 150°C and the tendency of quartz to be velocity weakening to ~300°C argues for unstable slip along fault zones in the 150°–300°C range, approximating the seismogenic zone. Quartz and granite frictional behavior are plotted together because quartz is a framework silicate and granite is dominated by framework silicates or quartz and feldspar.

depth. However, the ubiquitous presence of fluids in accretionary prisms may mediate the stress levels (see fluid pressures below).

In subduction zones, brittle deformation dominates to 150°–200°C. Brittle structures in accretionary prisms begin to be overprinted by ductile structures at ~150°–200°C. Rocks deformed in the 200°–300°C range commonly show ductile deformation, acting as pressure solution, repeatedly overprinted by brittle failure [*DiTullio and Byrne*, 1990; *Lewis and Byrne*, 2001; *Meneghini*, 2003; *Onishi and Kimura*, 1995; *Rowe and Moore*, 2003]. Microscopically, this alternation is seen as a pressure-solution fabric and as syntectonic growth of quartz fibers and other minerals that are cross cut by brittle fractures. Subsequently, the brittle-fracture phenomena are redeformed by pressure-solution fabrics (fig. 10.8). In rocks deformed at 300°C and above, there is little evidence for brittle deformation.

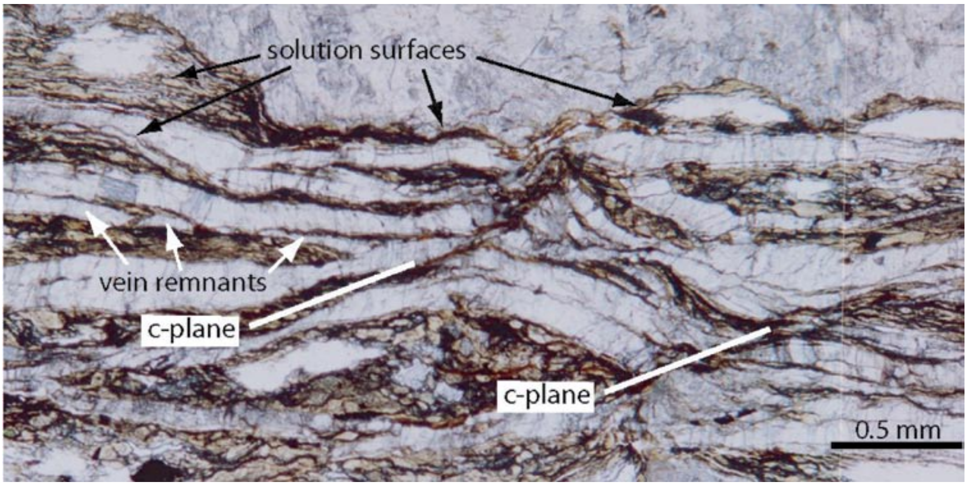

Figure 10.8 Veined fault surface showing interplay of solution and brittle fracture as vein emplacement. Light grey represents carbonate veins, whereas greenish layers are dominantly chlorite. Vein boundaries, especially large vein at top of figure, commonly modified by irregular pressure solution surfaces. Chloritic layers also show internal pressure solution surfaces. Note remnants of vein in upper right showing extreme solution effects resulting in boudinage of vein. Veins show varying degrees of disruption and modification by solution, suggesting veins of differing ages. Veins and pressure-solution fabric are approximately horizontal in photomicrograph. Pressure-solution fabric, in combination with shear surfaces, or "c-planes" define S-C fabric characteristic of shear zones. Photomicrograph from veined core of fault shown in figure 10.6 [*Meneghini*, 2003].

The apparently widespread alternation of pressure solution and brittle deformation in the 200º–300ºC range suggests an alternation of fluid pressure and/or differential stress. A low fluid pressure, low differential stress regime would favor pressure solution, whereas high fluid pressures and/or high differential stress could cause brittle failure. The pressure-solution regime represents relatively low strain rate interseismic deformation, as has been suggested elsewhere [*Duebendorfer et al.*, 1998; *Gratier and Gamond*, 1990]. The brittle deformation may be coseismic, although it could also represent fracture at less than seismic strain rates [*Cowan*, 1999].

How Does Fluid Pressure Vary Above and Into the Seismogenic Zone?

Background

Because pore pressure is one of the most critical controls on rock deformation, a principal goal of the proposed deep drilling into seismogenic zones is to measure pore pressure [*Kimura et al.*, 2003]. Shallow direct measurements of fluid pressures at the frontal part of accretionary prisms have yielded modest overpressuring [*Becker et al.*, 1997; *Screaton et al.*, 1995], and modeling suggests development of higher pressures at somewhat greater depths [*Bekins and Dreiss*, 1992; *Saffer and Bekins*, 1998]. Moreover, both frontal thrusts [*Le Pichon et al.*, 1987; *Moore et al.*, 1990] and out-of-sequence thrusts [*Shipboard Scientific Party*, 1994] are known to seep fluid at the surface, thus indicating they are conduits of active fluid flow that are be overpressured. The onset of high fluid pressures at depths <3–4 km is due to the rapid consolidation of sediments at shallow depths [e.g., *Screaton et al.*, 2002]. Also, mineral phase transitions including smectite to illite and opal to quartz transformations may contribute to overpressuring [*Moore and Vrolijk*, 1992]. The wide distribution of high fluid pressures suggested by the models coupled with the low state of consolidation and lithification of the sediments may explain the lack of seismicity at the depths of <4 km in sediment-dominated accretionary prisms. The disappearance of the décollement as a clear reflector at seismogenic depths in the Nankai accretionary prism has been attributed to dewatering and presumably depressurization of the sediment underthrust below the décollement [*Bangs et al.*, 2004].

Observations from Subaerially Exposed Accretionary Prisms

Uplifted accretionary prism rocks provide a record of elevated fluid pressures preserved in both the fluid inclusions and geometry of veins and cements. Studies of fluid inclusions in shear and extensional veins of accretionary prisms show high and variable fluid pressures that are interpreted to be near lithostatic [*Lewis et al.*, 2000; *Vrolijk*, 1987]. *Vrolijk* [1987] suggested that the quartz vein growth was associated with a phase of major fluid movement along the décollement of the accretionary prism and that it initiated at the high range of observed fluid pressures and cyclically decreased through time. On the basis of low wall rock porosities and the discontinuous and limited occurrence of veins, *Lewis and Byrne* [2003; *Lewis et al.*, 2000] suggest that the observed veins reflect a small amount of fluid trickling through a previously emplaced accretionary prism, albeit at fluid pressures 75% of lithostatic or higher.

Extensive veining paralleling a shallowly dipping latest Cretaceous accretionary thrust in the Marin Headlands of northern California (fig. 10.6) indicates that fluid pressures were sufficient to open cracks perpendicular to the minimum principal stress plus any tensional strength of the rock [*Meneghini*, 2003]. Because this was a shallowly dipping accretionary thrust and the veins parallel it, the veins would have required a fluid pressure at least equal to the overburden. The zone of extensional veining is ~40 m thick along the thrust surface (fig. 10.6). The extraordinary quantity of veins in the fault zone suggests copious fluid flow. Cross-cutting relationships suggest generations of veining, brittle fracture, and pressure solution. Together these structures indicate alternation of compression and dilation across the fault surface that may represent fault-valve behavior and may be tied to the seismic cycle [*Meneghini,* 2003]. Apparently, the 40-m-thick zone of veins developed cumulatively with only a portion being active at any time. A 40-m thickness of dilated fault might be seismically resolvable at this depth. A thin dilated zone would not be imaged if it were less than ~10 m thick. Thus this fault zone may be a good analogue for the area downdip along the Nankai décollement where the reflection disappears [*Bangs et al.,* 2004].

Overall, fluid pressures appear to be high and broadly distributed in time and space at shallow depths due to the intergranular fluid sources, mineral phase changes, and hydrocarbon generation that produce fluids. At greater depths the fluid pressures also apparently transiently high, and the conduits of flow are more localized along faults owing to the reduction of intergranular permeability resulting from the consolidation and low-grade metamorphism in the accretionary prism [*Lewis and Byrne,* 2003]. As prism rocks are buried deeper than ~5 km, porosity changes are small [*Bray and Karig,* 1985]; hence fluids are probably derived primarily from continuing mineral dehydration reactions [*Hacker et al.,* 2003].

Strain Localization

In accretionary prisms the early faults are characterized by broader zones of scaly mudstone and stratal disruption, shear bands, and minor faults [*Shipboard Scientific Party*, 1991]. Faults developed later in consolidated prism interiors are more discrete than earlier primary accretionary structures (fig. 10.9). Experimental studies suggest that localized deformation on discrete, throughgoing shear surfaces tends to be of lower strength and more likely to be velocity weakening than distributed deformation in broader shear zones [*Beeler et al.,* 1996; *Marone,* 1998].

On a large scale in accretionary prisms it appears that shear strain localization in the form of out-of-sequence thrusts approximately correlates with the seaward limit of modeled earthquake displacements and onset of recorded microearthquakes in the Nankai Trough (fig. 10.10) [*Obana et al.,* 2003; *Park et al.,* 2000]. This implies that the consolidation/lithification processes in the prism are allowing it to deform as discrete large-scale blocks with slip localized along the out-of-sequence thrusts [*Lewis and Byrne,* 2003]. Out-of-sequence thrusts are clearly defined in ancient prisms and tend to partition them into packages with differing sedimentary, structural, or metamorphic history (fig. 10.11). The demonstrated activity of these out-of-sequence thrusts in past great earthquakes indicates a significant role in releasing seismic energy [*Pflaker,* 1972]. Moreover, modern activity of out-of-sequence thrusts suggests major activity near the frontal part of the accretionary prism and quiescence in a landward portion of the prism (fig. 10.11).

(a)

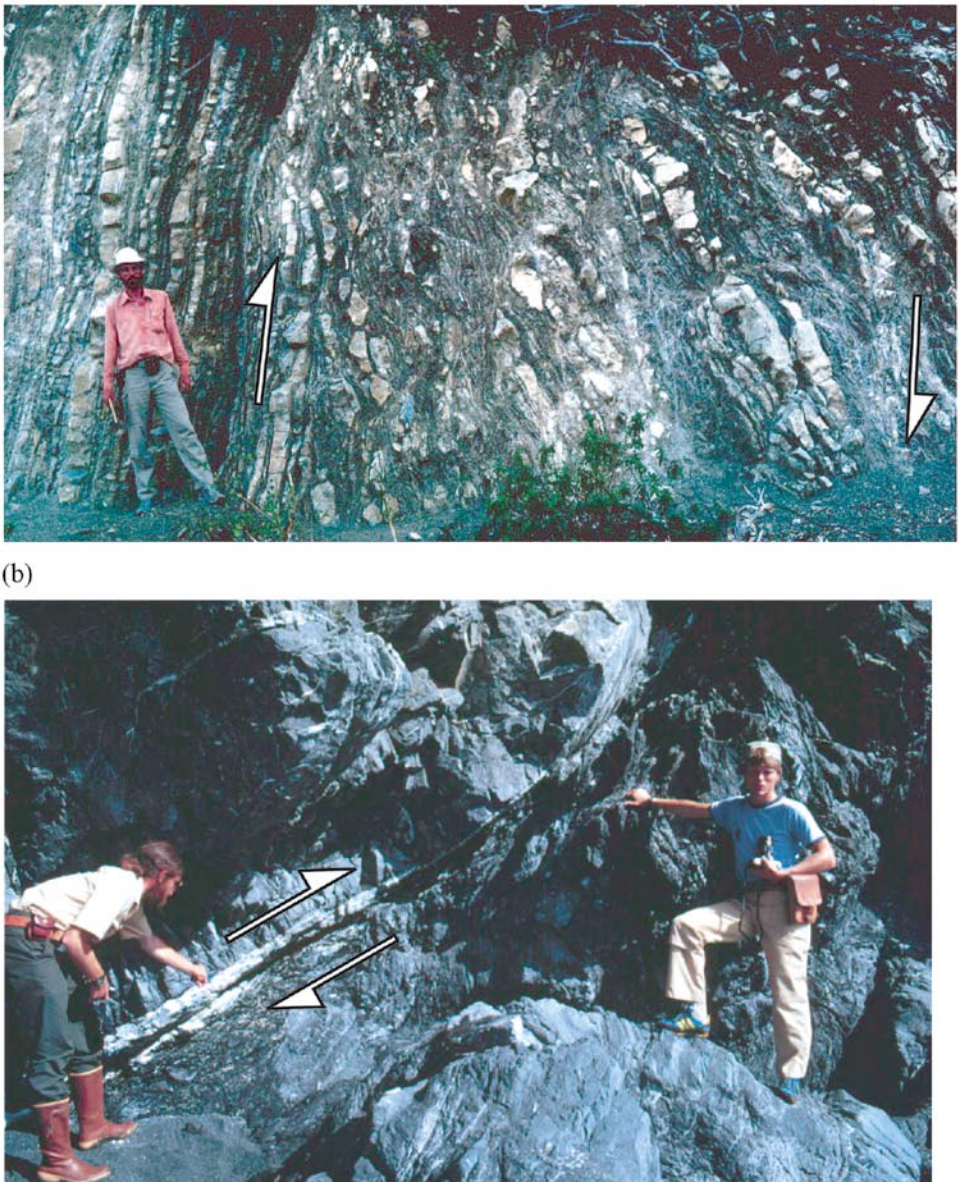

Figure 10.9 Outcrop examples of distributed faulting verses shear localization in accretionary prisms. (a) Outcrop of a stratally disrupted fault zone, Eocene accretionary prism, Dominican Republic [*Witschard and Dolan*, 1990]. Broad zone of deformation continues at least 10 m right beyond the edge of the photo. Inclined fabric of disruption zone indicates stratified rocks, where Jim Dolan is standing, are up relative to the disrupted rocks. (b) Discrete out-of-sequence thrust fault cutting early steeply dipping stratally disrupted fabric (beneath Peter Vrolijk's feet, right); note white quartz vein in fault being pointed to by Tim Byrne (left). Paleocene accretionary prism, Kodiak Islands Alaska.

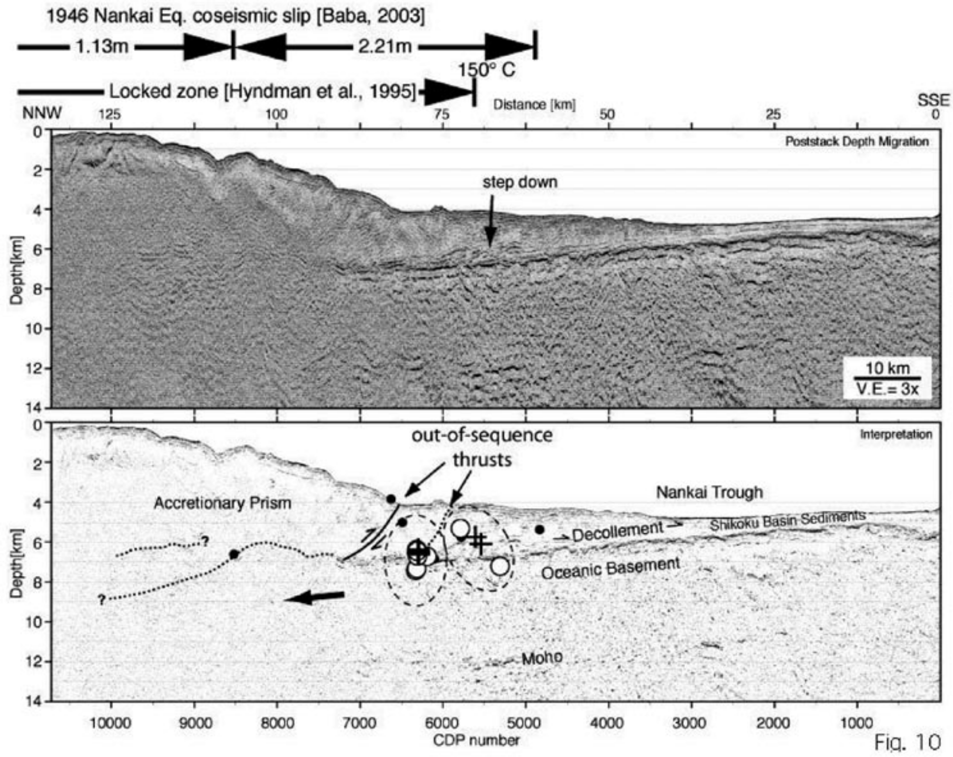

Figure 10.10 Seismic reflection depth section with nearby microearthquakes projected on to it [*Obana et al.*, 2003]. Note that microearthquakes die out just seaward of the initial development of out-of-sequence thrusts. Note also that the accretionary prism has a shallow even taper in its seaward extent, but the surface slope begins to steepen and become more irregular landward of the development of the out-of-sequence thrusts and the onset of seismicity.

Development of Upper-Plate Rigidity

The sudden slip during an earthquake results from the release of strain accumulated in rock masses on either side of the fault [e.g., *Scholz*, 2002, pp. 244–247]. Subduction thrusts beneath accretionary prisms are unique in that the upper plate begins as poorly consolidated, overpressured sediment with insufficient elastic strength to accumulate strain [*Byrne et al.*, 1988]. Even if the mechanical properties of the fault surface evolve to support unstable slip, the upper plate must develop sufficient elastic strength to produce the slip event. The accretionary prism thickens landward as required for its continued growth [*Davis et al.*, 1983]; owing to their progressive burial, the included rocks undergo consolidation, metamorphism, and cementation acquiring elastic strength. The onset of seismic activity typically occurs where the overlying prism has minimum thickness of 3–5 km and typically at localities with a high thermal

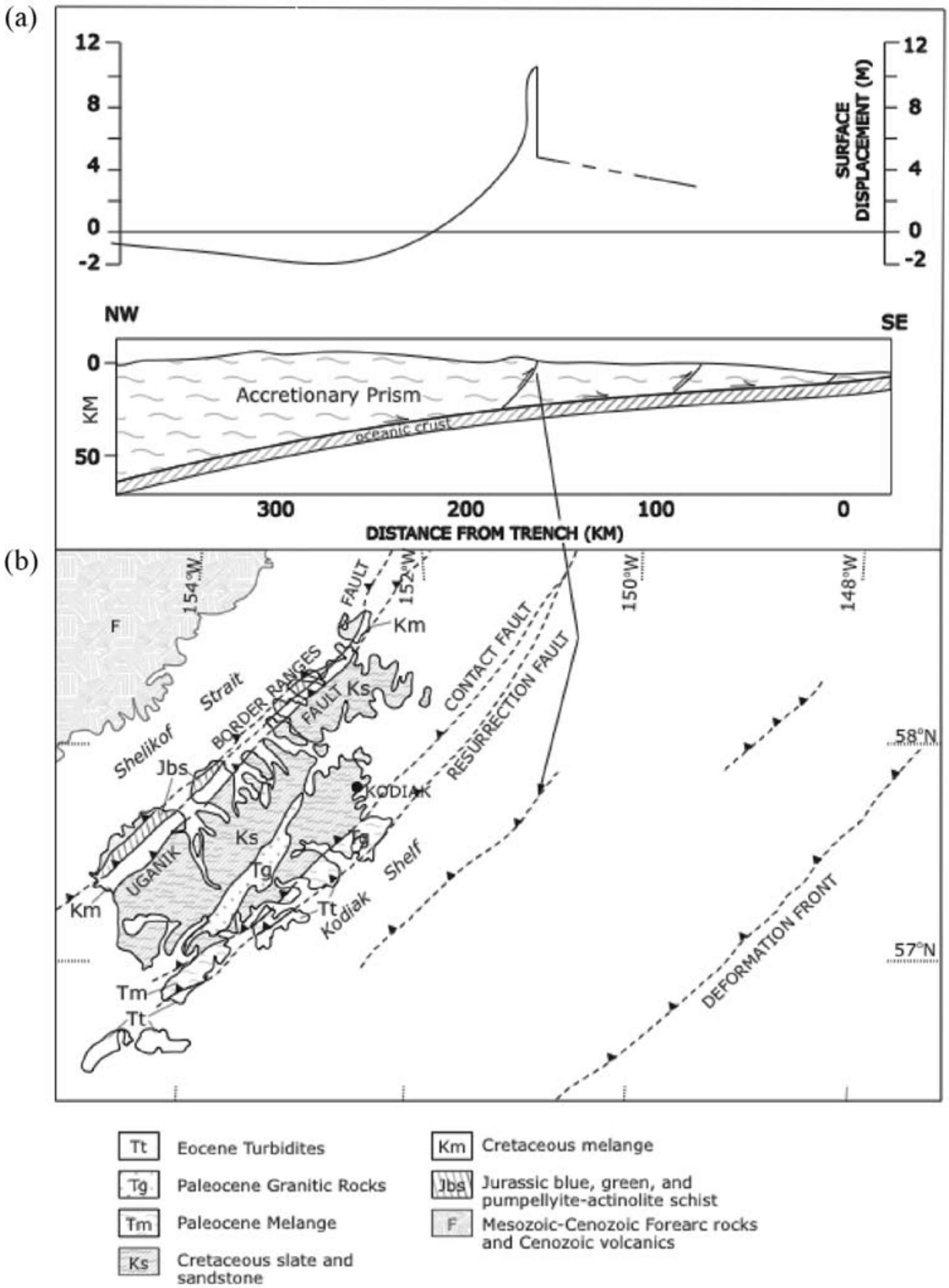

Figure 10.11 (a) Map showing thrust faults cutting accretionary prism [*Moore et al.*, 1991; *Plafker*, 1972; *Plafker et al.*, 1994]. All but frontal thrust is out-of-sequence thrusts. (b) Cross section from Prince William Sound, just north of the area shown in figure 10.11a, showing correlation to fault that was active during 1964 earthquake [*Plafker*, 1972]. Faults seaward of the correlated fault were inferred to be active during the 1964 earthquake. Seismic reflection data show that these faults deform young sediments at the seafloor.

gradient [*Obana et al.*, 2003; *Bilek and Lay,* 2000]. Apparently, the high thermal gradients accelerate metamorphism, cementation, and rigidification of the upper plate.

Summary

Accretionary prisms develop by the underthrusting and emplacement of rocks carried by the downgoing plate. Aside from those materials scraped off at the deformation front, all rocks that are underthrust more deeply must descend beneath the décollement, and experience the décollement step-down through or around them, thus achieving accretion to the upper plate. Thus, depending on their depth of accretion, these rocks preserve a record of deformation in the upper aseismic zone, the seismogenic zone, and the lower aseismic zone. Drawing from the consensus of thermal models of modern seismicity in subduction zones, we define prism rocks of the upper aseismic zone as those emplaced at temperatures of <125°C, of the seismogenic zone as those that have been subjected to temperatures of 125º–350°C, and those of the lower aseismic zone as those emplaced at temperatures >350°C. These temperature limits are approximate and transitional with errors of about ±15–20%. They apply to continental margin, not oceanic subduction zone settings. As sediments and rocks are emplaced at differing temperatures and depths, they acquire specific rheologically significant metamorphic and deformational imprints:

1. During initial burial to ~125°C, accretionary prism sediments become rocks, undergoing diagenetic reactions including of the transformation of smectite to illite, the albitization of detrital feldspar, dehydration of opal, and hydrocarbon generation. Although the smectite to illite transition does increase the coefficient of friction or strength, illite's rate-dependent friction is velocity strengthening and not subject to accelerating slip. However, the cations (calcium, magnesium, iron) released during the smectite to illite transition and the albitization process foster cementation.

2. Cementation and veining by carbonates becomes common above 125°C, perhaps owing to the above-mentioned release of cations. Pressure-solution fabrics begin to be apparent at ~150°C, with well-developed cleavages and quartz veining common by 200°C. Pressure solution may be facilitated by the diagenetic formation of illite and its catalyzing effect on quartz and feldspar dissolution.

3. Quartz veining and cementation in the 150º–300°C range facilitate the change from a velocity-strengthening to a velocity-weakening, earthquake-prone rheology.

4. Cementation by quartz and carbonates increases cohesion and may also make the rocks subject to unstable failure.

5. In accretionary prisms, brittle fabrics are progressively replaced by ductile fabrics through a temperature range of ~150°–325°C.

6. Although rocks in the seismogenic zone have lost most of their intergranular fluid through consolidation, vein geometries and fluid inclusions suggest high fluid pressures, approximately at lithostatic.

7. Strain localization in the formation of discrete faults occurs across the lower aseismic to seismic transition. Strain localization is observed both at microscopic, outcrop, and map scale. Active out-of-sequence thrusts occur in the frontal portions of accretionary prisms and represent a map-scale example of strain localization and seismic behavior.

The evolution of the accretionary prism from aseismic to seismic behavior involves the changes in material properties from fault zones dominated by clays to those in which quartz and carbonate are introduced by diffusion and fluid advection. Although both the quartz and carbonate increase cohesion, only quartz displays a velocity-weakening frictional response. The rate-dependent frictional behavior of carbonate is not well defined.

Consolidation, cementation, and other diagenetic-metamorphic transitions of the accretionary prism lead to the development of an upper plate of the subduction zone with increasing elastic strength. Development of this rigid upper plate is a prerequisite for plate-boundary seismicity because stick-slip behavior requires that both the hanging wall and foot wall of a fault store elastic strain energy. The seawardmost out-of-sequence thrusts define the seaward edge of this elastically rigid block.

Acknowledgments

We thank Peter Eichhubl and Jim Boles for helpful discussions on diagenesis and low-grade metamorphism. Sampling access to the outcrops in Marin Headlands provided by the National Park Service. We thank Jon Lewis and Tim Byrne for helpful reviews that clarified the text. Koichiro Obana provided a high-quality copy of figure 10.11 and American Geophysical Union granted permission for its reproduction here. Research supported by NSF grants OCE-9802264 and OCE-0203664 and Italian government grant M.I.U.R. COFIN 2003.

References

Aydin, A. (1978), Small faults as deformation bands in sandstone, *Pure Appl. Geophys.*, *116*, 913–930.

Bangs, N., S. Shipley, G. Moore, S. Gulick, S. Kuromoto, and Y. Nakamura (2004), Evolution of the Nankai Trough décollement from the trench into the seismogenic zone: Inferences from three-dimensional seismic reflection imaging, *Geology*, *32*(4), 273–276.

Becker, K., A. T. Fisher, and E. E. Davis (1997), The CORK experiment in Hole 949C: long-term observations of pressure and temperature in the Barbados accretionary prism, *Proc. Ocean Drill. Program Sci. Results, 156,* 239–252.

Beeler, N. M., et al. (1996), Frictional behavior of large displacement experimental faults, *J. Geophys. Res.*, *101*, 8697–8715.

Behl, R. J., and R. E. Garrison (1994), The origin of chert in the Monterey Formation of California (USA), in *Siliceous, Phosphatic and Glauconitic Sediments of the Tertiary and Mesozoic*, edited by A. Iijima and Garrison, pp. 101–132, VSP, Int. Sci.,Utrecht, Netherlands.

Bekins, B., and S. Dreiss (1992), A simplified analysis of parameters controlling dewatering in accretionary prisms, *Earth Planet. Sci. Lett.*, *109*, 275–287.

Bilek, S. L., and T. Lay (2000), Depth dependent rupture properties in circum-Pacific subduction zones, in *Geocomplexity and the Physics of Earthquakes*, *Geophys. Monogr. Ser*., vol. 120, edited by J. B. Rundle, D. L. Turcott, and W. Klein, pp. 165–186, AGU, Washington, D.C.

Bjorkum, P. A. (1996), How important is pressure in causing dissolution of quartz in sandstone? *J. Sediment. Res.*, *66*, 147–154.

Blake, M. C. J., R. W. Graymer, and D. L. Jones (2000), Geologic map and map database of parts of Marin, San Francisco, Alameda, Contra Costa, and Sonoma counties, California, *U.S. Geol. Surv. Miscell. Field Stud., MF-2337*.

Blanpied, M. L., D. A. Lockner, and J. D. Byerlee (1995), Frictional slip of granite at hydrothermal conditions, *J. Geophys. Res.*, *100*, 13,045–13,064.

Boles, J. R. (1982), Active albitization of plagioclase, Gulf Coast Tertiary, *Am. J. Sci.*, *282*, 165–180.

Boles, J. R., and S. G. Franks (1979), Clay diagenesis in Wilcox sandstones of southwest Texas—Implications of smectite diagenesis on sandstone cementation, *J. Sediment. Petrol.*, *49*, 55–70.

Brandon, M. T., and J. A. Vance (1992), Tectonic evolution of the Cenozoic Olympic subduction complex, Washington State, as deduced from fission track ages for detrital zircons, *Am. J. Sci.*, *292*, 564–636.

Bray, C. J., and D. E. Karig (1985), Porosity of sediments in accretionary prisms and some implications for dewatering processes, *J. Geophys. Res.*, *90*, 768–778.

Byrne, D. E., D. M. Davis, and L. R. Sykes (1988), Loci and maximum size of thrust earthquakes and the mechanics of the shallow region of subduction zones, *Tectonics*, *7*, 833–857.

Byrne, T. (1984), Early deformation in melange terranes of the Ghost Rocks Formation, Kodiak Islands, Alaska, *Spec. Pap. Geol. Soc. Am., 198*, 21–52.

Byrne, T. (1998), Seismicity, slate belts and coupling along convergent plate boundaries, *Eos Trans. AGU*, *79*, W-114.

Byrne, T., A. J. Maltman, E. Stephenson, and W. Soh (1993), Deformation structures and fluid flow in the toe region of the Nankai accretionary prism, *Proc. Ocean Drill. Program Sci. Results*, *131*, 83–101.

Cowan, D. S. (1999), Do faults preserve a record of seismic slip? A field geologist's opinion, *J. Struct. Geol.*, *21*, 995–1001.

Currie, C. A., R. D. Hyndman, K. Wang, and V. Kostoglodov (2002), Thermal models of the Mexico subduction zone: Implications for the megathrust seismogenic zone, *J. Geophys. Res.*, *107*(B12), 2370, doi:10.1029/2001JB000886.

Davis, D. J., J. Suppe, and F. A. Dahlen (1983), Mechanics of fold-and-thrust belts and accretionary wedges, *J. Geophys. Res.*, *88*, 1153–1172.

Di Toro, G., D. L. Goldsby, and T. E. Tullis (2004), Friction falls towards zero in quartz rock as slip velocity approaches seismic rates, *Nature*, *427*, 436–439.

DiTullio, L., and T. Byrne (1990), Deformation paths in the shallow levels of an acccretionary prism: The Eocene Shimanto belt of southwest Japan, *Geol. Soc. Am. Bull.*, *102*, 1420–1438.

DiTullio, L., M. Laughland, and T. Byrne (1993), Thermal and constraints on deformation from illite crystallinity and vitrinite relfectance in shallow levels of an acretionary prism Eocene-Oligocene Shimanto Belt, southwest Japan, in *Thermal Evolution of the Tertiary Shimanto Belt, Southwest Japan: An Example of Ridge-Trench Interaction*, edited by M. B. Underwood, *Spec. Pap. Geol. Soc Am.*, *273*, 63–82,

Duebendorfer, E. M., J. Vermilye, P. A. Beiser, and T. L. Davis (1998), Evidence for aseismic deformation in the western Transverse Ranges, southern California; implications for seismic risk assessment, *Geology*, *26*(3), 271–274.

Ernst, W. G. (1990), Thermobarometric and fluid expulsion history of subduction zones, *J. Geophys. Res.*, *95*, 9047–9053.

Feehan, J., and M. T. Brandon (1999), Contribution of ductile flow to exhumation of low-T-high-*P* metamorphic rocks: San Juan-Cascade nappes, NW Washington State, *J. Geophys. Res.*, *104*, 10,883–810,902.

Fisher, D., and T. Byrne (1987), Structural evolution of underthrusted sediments, Kodiak Islands, Alaska, *Tectonics*, *6*, 775–794.

Fisher, D., and T. Byrne (1992), Strain variations in an ancient accretionary complex: implications for forearc evolution, *Tectonics*, *11*, 330–347.

Fisher, D. M. (1996), Fabrics and veins in the forearc: A record of cyclic fluid flow at depths of <15 km, in *Subduction Top to Bottom*, *Geophys. Monogr. Ser.*, vol. 96, edited by J. P. Platt, pp. 75–89, AGU, Washington, D. C.

Fisher, D. M., and S. L. Brantley (1993), Models of quartz overgrowth and vein formation: Deformation and fluid flow in an ancient subduction zone, *J. Geophys. Res.*, *97*, 20,043–20,061.

Geddes, D. (1993), Carbonate cement in sandstone as an indicator of accretionary complex hydrogeology, M.S. thesis, 107 pp., Univ. of Calif., Santa Cruz.

Gratier, J. P., and J. F. Gamond (1990), Transition between seismic and aseismic deformation in the upper crust, in *Deformation Mechanisms, Rheology and Tectonics,* edited by R. J. Knipe and E. H. Rutter, *Spec. Publ. Geol. Soc. London*, *54*, 461–473.

Hacker, B. R., G. A. Abers, and S. M. Peacock (2003), Subduction factory: 1. Theoretical mineralogy, densities, seismic wave speeds, and H_2O contents, *J. Geophys. Res.*, *108*(B1), 2029, doi:10.1029/2001JB001127.

Helper, M. A. (1986), Deformation and high P/T metamorphism in the central part of the Condrey Mountain window, north-central Klamath Mountains, California and Oregon, in *Blueschists and Eclogites*, edited by B. W. Evans and E. H. Brown, *Mem. Geol. Soc. Am.*, *164*, 107–123.

Hibbard, J. P., M. M. Laughland, S. M. Kang, and D. Karig (1993), The thermal imprint of spreading ridge subduction on the upper levels of an accretionary prism, Southwest Japan, in *Thermal Evolution of the Tertiary Shimanto Belt, Southwest Japan: An Example of Ridge-Trench Interaction*, edited by M. B. Underwood, pp. 83–101, Geol. Soc. of Am., Boulder Colo.

Hunt, J. M. (1996), *Petroleum Geochemistry and Geology,* 2nd ed., 743 pp., W. H. Freeman, New York.

Hyndman, R. D. (1997), Seismogenic zone of subduction thrust faults, *Island Arc*, *6*, 244–260.

Hyndman, R. D., and K. Wang (1993), Thermal constraints on the zone of major thrust earthquake failure: The Cascadia subduction zone, *J. Geophys. Res.*, *98*, 2039–2060.

Hyndman, R. D., M. Yamano, and D. A. Oleskevich (1997), The seismogenic zone of subduction thrust faults, *Island Arc*, *6*, 224–260.

Ikesawa, E., A. Sakaguchi, and G. Kimura (2003), Pseudotachylyte from an ancient accretionary complex: Evidence for melt generation during seismic slip along a master décollement, *Geology*, *31*(7), 637–640.

Isaacs, C. M., K. A. Pisciotto, and R. E. Garrison (1983), Facies and diagenesis of the Miocene Monterey Formation, California: A summary, in *Siliceous Deposits in the Pacific Region, Developments in Sedimentology,* vol. 36, edited by A. Iijima, J. R. Hein, and R. Siever, pp. 247–282, Elsevier, New York.

Jayko, A. S., M. C. J. Blake, and R. N. Brothers (1986), Blueschist metamorphism of the Eastern Franciscan belt, northern California, *Mem. Geol. Soc. Am.*, *164*, 107–123.

Kimura, G., and A. Mukai (1990), Underplated units in an accretionary complex: Melange of the Shimanto Belt of eastern Shikoku, southwestern Japan, *Tectonics*, *10*, 31–50.

Kimura, G., H. Tobin, and N. W. Group (2003), NanTroSEIZE: The Nankai Trough Seismogenic Zone Experiment Complex Drilling Project, report, p. 33, N. M. Tech, Socorro.

Kitamura, Y., K. Sato, E. Ikesawa, K. Ikehara-Ohmori, G. Kimura, H. Kondo, K. Ujiie, C. T. Onishi, K. Kawabata, Y. M. H. Hashimoto, and H. Masago (2005), Melange and its seismogenic roof decollement: A plate boundary fault rock in the subduction zone- An example from the Shimanto Belkt, Japan, *Tectonics, 24*, p. TC5012, doi:10.1029/2004TX001635, 2005.

Kulm, L. D., and E. Suess (1990), The relation of carbonate deposits to fluid venting processes: Oregon accretionary prism, *J. Geophys. Res.*, *95*, 8899–8915.

Kusky, T. M., and D. C. Bradley (1999), Kinematic analysis of Mélange fabrics: Examples and applications from the McHugh Complex, Kenai Peninsula, Alaska, *J. Struct. Geol.*, *21*, 1773–1796.

Labaume, P., M. Kastner, A. Trave, and P. Henry (1997), Carbonate veins from the decollement zone at the toe of the Northern Barbados accretionary prism: microstructure, mineralogy, geochemistry and relations with prism structures and fluid regime, *Proc. Ocean Drill. Program Sci. Results*, *156*, 79–96.

Lay, T., and S. Bilek (2007), Anomalous earthquake ruptures at shallow depths on subduction zone megathrusts, this volume.

Le Pichon, X., et al. (1987), Nankai Trough and Zenisu Ridge: A deep-sea submersible survey, *Earth Planet. Sci. Lett.*, *83*, 285–299.

Lewis, J. C., and T. Byrne (2001), Fault kinematics and past plate motions at a convergent plate boundary: Tertiary Shimanto Belt, southwest Japan, *Tectonics*, *20*, 548–565.

Lewis, J. C., and T. Byrne (2003), History of metamorphic fluids along outcrop-scale faults in a Paleogene accretionary prism, SW Japan: Implications for prism-scale hydrology, *Geochem. Geophys. Geosyst.*, *4*, 9007, doi:10.1029/2002GC000359.

Lewis, J. C., T. Byrne, J. D. Pasteris, D. London, and G. B. I. Morgan (2000), Early Tertiary fluid flow and pressure-temperature conditions in the Shimanto accretionary complex of south-west Japan: Constraints from fluid inclusions, *J. Metamorphic Geol.*, *18*, 319–333.

Lewis, J. C., J. R. Unruh, and R. J. Twiss (2003), Seismogenic strain and motion of the Oregon coast block, *Geology*, *31*(22), 183–186.

Lockner, D. A., and J. Byerlee (1986), Laboratory measurements of velocity-dependent friction strength, *U.S. Geol. Surv. Open File Rep., 86–417*.

Lucas, S. E., and J. C. Moore (1986), Cataclastic deformation in accretionary prisms: DSDP Leg 66, and onland examples from Barbados and Kodiak Islands, in *Structural Fabrics From Deep Sea Drilling Project Cores From Forearcs*, edited by J. C. Moore, *Mem. Geol. Soc. Am.* , *166*, 89–103.

Maltman, A. J., T. Byrne, D. E. Karig, S. J. Lallemant, R. Knipe, and D. Prior (1993), Deformation structures at Site 808, Nankai accretionary prism, Japan, *Proc. Ocean Drill. Program Sci. Results*, *131*, 123–133.

Maltman, A. J., P. Labaume, and B. Housen (1997), Structural geology of the decollement at the toe of the Barbados accretionary prism, *Proc. Ocean Drill. Program Sci. Results*, *156*, 279–292.
Marone, C. (1998), Laboratory-derived friction laws and their application to seismic faulting, *Annu. Rev. Earth Planet. Sci.*, *26*, 643–696.
Meneghini, F. (2003), Hydrofracture, fluid flow and deformation in fossil accretionary prisms: The examples on the Internal Ligurian Units (northern Apennines, Italy) and the Franciscan Complex (California Coast Ranges, N. California, USA), Ph.D. thesis, 174 pp, Univ. of Pisa, Pisa, Italy.
Moore, G. W. (1980), Slickensides in deep sea cores near the Japan Trench, Leg 57, Deep Sea Drilling Project, *Initial Rep. Deep Sea Drill. Proj.*, *56–57*, part 2, 1107–1116.
Moore, J. C. (Ed.) (1986), *Structural Fabrics in Deep Sea Drilling Project Cores From Forearcs*, *Mem. Geol. Soc. Am.*, *166*, 160 pp.
Moore, J. C., and A. Allwardt (1980), Progressive deformation of a Tertiary trench slope, Kodiak Islands, Alaska, *J. Geophys. Res.*, *85*, 4741–4756.
Moore, J. C., and P. Vrolijk (1992), Fluids in accretionary prisms, *Rev. Geophys.*, *30*, 113–135.
Moore, J. C., D. L. Orange, and L. D. Kulm (1990), Interrelationship of fluid venting and structural evolution: Alvin observations from the frontal accretionary prism, Oregon, *J. Geophys. Res.*, *95*, 8795–8808.
Moore, J. C., F. Diebold, M., V. H. Sample, R., T. Brocher, B. Page, D. Stone, M. Talwani, J. Ewing, C. Rowe, and J. Davies (1991), EDGE deep seismic reflection transect of the eastern Aleutian arc-trench layered lower crust reveals underplating and continental growth, *Geology*, *19*(5), 420–424.
Morrow, C. A., B. Radney, and J. Byerlee (1992), Frictional strength and the effective pressure law of montmorillonite and illite clays, in *Fault Mechanics and Transport Properties of Rocks*, edited by Evans, B., and T. F. Wong, pp. 69–88, Academic Press, San Diego.
Muhuri, S. K., T. A. Dewers, E. S. J. Thurmann, and Z. Reches (2003), Interseismic fault strengthening and earthquake-slip instability: Friction or cohesion, *Geology*, *31*(10), 881–884.
Mullis, J., J. Dubessy, B. Poty, and J. O'Neil (1994), Fluid regimes during late stages of a continental collision: Physical, chemical, and stable isotope measurements of fluid inclusions in fissure quartz from a geotraverse through the Central Alps, Switzerland, *Geochim. Cosmochim. Acta*, *58*, 2239–2267.
Norabuena, E., et al. (2004), Geodetic and seismic constraints on some seismogenic zone processes in Costa Rica, *J. Geophys. Res.*, *109,* B11403, doi:10.1029/2003JB002931.
Norris, R. J., and D. G. Bishop (1990), Deformed conglomerates and textural zones in the Otago Schists, South island, New Zealand, *Tectonophysics*, *174*, 331–349.
Obana, K., et al. (2003), Microseismicity at the seaward updip limit of the western Nankai Trough seismogenic zone, *J. Geophys. Res.*, *108(*B10), 2459, doi:10.1029/2002JB002370.
Oleskevich, D. A., R. D. Hyndman, and K. Wang (1999), The updip and downdip limits to great subduction earthquakes: Thermal and structural models of Cascadia, south Alaska, SW Japan, and Chile, *J. Geophys. Res.*, *104*, 14,965–14,991.
Onishi, C. T., and G. Kimura (1995), Change in fabric of melange in Shimanto Belt, Japan: Change in relative convergence? *Tectonics*, *14*, 1273–1289.
Orange, D. L., and M. B. Underwood (1995), Patterns of thermal maturity as diagnostic criteria for interpretation of melanges, *Geology*, *23*(12), 1144–1148.
Orange, D. L., D. S. Geddes, and J. C. Moore (1993), Structural and fluid evolution of a young accretionary complex; the Hoh rock assemblage of the western Olympic Peninsula, Washington, *Geol. Soc. Am. Bull.*, *105*, 1053–1075.
Park, J. O., et al. (2000), Out-of-sequence thrust faults developed in the coseismic slip zone of the 1946 Nankai earthquake (M_w = 8.2) off Shikoku, southwest Japan, *Geophys. Res. Lett.*, *27*, 1033–1036.

Peacock, S. M. (1993), The importance of blueschist ~~e~~clogite dehyration reactions in subducting oceanic crust, *Geol. Soc. Am. Bull.*, *105*, 684–694.

Plafker, G. (1972), Alaskan earthquake of 1964 and Chilean earthquake of 1960: Implications for arc tectonics, *J. Geophys. Res.*, *77*, 901–925.

Plafker, G., J. C. Moore, and G. R. Winkler (1994), Geology of the southern Alaska margin, in *The Geology of Alaska*, edited by P. G. and H. C. Berg, pp. 389–449, Geol. Soc. of Am., Boulder, Colo.

Ring, U., and M. T. Brandon (1999), Ductile deformation as mass loss in the Franciscan Subduction Complex: Implications for exhumation processes in accretionary wedges, in *Ehumation Processes: Normal Faulting, Ductile Flow, and Erosion*, edited by U. Ring et al., pp. 55–86, Geol. Soc., London.

Roeske, S. (1986), Field relations and metamorphism of the Raspberry Schist, Kodiak Islands, Alaska, in *Blueschist and Eclogites*, edited by B. W. Evans and E. H. Brown*, Mem. Geol. Soc. Am.*, *164*, 169–184.

Rowe, C., E. Thompson, and J. C. Moore (2002), Contrasts in faulting and veining across the aseismic to seismic transition, Kodiak Accretionary Complex, Alaska, *Eos Trans. AGU, 83*(47), Fall Meet. Suppl., Abstract T21A-1060.

Rowe, C., J. C. Moore, F. Meneghini, and A. W. McKiernan (2005), Large-scale pseudotachylytes and fluidized cataclasites from an ancient subduction thrust fault, *Geology*, *33*(12), 937–940.

Rowe, C. D., and J. C. Moore (2003), The upper aseismic to seismic transition: A silica mobility threshold, *Eos Trans. AGU*, *84*(46), Fall Meet. Suppl., Abstract T41E-02.

Saffer, D., and C. Marone (2003), Comparisons of smectite and illite-rich gouge, frictional properties: applications to the updip limit of the seismogenic zone of subduction thrusts, *Earth and Planetary Science Letters, 215*, 219–235.

Saffer, D. M., and B. A. Bekins (1998), Episodic fluid flow in the Nankai accretionary complex: Timescale, geochemistry, flow rates, and fluid budget, *J. Geophys. Res.*, *103*, 30,351–330,370.

Sample, J. C., and J. C. Moore (1987), Structural style and kinematics of an underplated slate belt, Kodiak Islands, Alaska, *Geol. Soc. Am. Bull.*, *99*, 7–20.

Sample, J. S. (1990), The effect of carbonate cementation of underthrust sediments on deformation styles during underplating, *J. Geophys. Res.*, *95*, 9111–9121.

Scholz, C. H. (2002), *The Mechanics of Earthquakes and Faulting*, 2nd ed., 471 pp., Cambridge Univ. Press, New York.

Schwartz, S., and B. Stockhert (1996), Pressure solution in siliciclastic HP-LT metamorphic rocks—Constraints on the state of stress in deep levels of accretionary complexes, *Tectonophysics*, *255*, 203–209.

Schwartz, S. Y., and H. R. DeShon (2007), Distinct updip limits to geodetic locking and microseismicity at the northern Costa Rica seismogenic zone: Evidence for two mechanical transitions, this volume.

Screaton, E. J., B. Carson, and G. P. Lennon (1995), Hydrologic properties of a thrust fault within the Oregon accretionary prism, *J. Geophys. Res.*, *100*, 20025–20035.

Screaton, E. J., et al. (2002), Porosity loss within the underthrust sediments of the Nankai accretionary complex; implications for overpressures, *Geology*, *30*(1), 19–22.

Shipboard Scientific Party (1991), Site 808, in *Proc. Ocean Drill. Program Initial Reports*, edited by Tiara, A., et al., v. 131, pp. 71–269, (Ocean Drilling Program), College Station, TX.

Shipboard Scientific Party (1994), Site 892, in *Proc. Ocean Drill. Program Initial Reports*, *146*, Part 1, 301–378.

Sibson, R. H. (1975), Generation of pseudotachylyte by ancient seismic faulting, *Geophys. J. R. Astron. Soc.*, *43*, 775–794.

Speed, R. (1990), Volume loss and defluidization history of Barbados, *J. Geophys. Res.*, *95*, 8983–8996.

Taira, A., J. Katto, M. Tashiro, M. Okamura, and K. Kodama (1988), The Shimanto Belt in Shikoku Japan: Evolution of a Cretaceous to Miocene accretionary prism, *Mod. Geol.*, *12*, 5–46.

Twiss, R. J., and E. M. Moores (1992), *Structural Geology*, 532 pp., W. H. Freeman, New York.

van der Pluijm, B. A., and S. Marshak (1997), *Earth Structure: An Introduction to Structural Geology and Tectonics*, 495 pp., McGraw-Hill, New York.

van der Pluijm, B. A., and S. Marshak (2004), *Earth Structure: An Introduction to Strutural Geology and Tectonics*, 656 pp., W.W. Norton, New York.

Vrolijk, P. J. (1987), Tectonically-driven fluid flow in the Kodiak accretionary complex, Alaska, *Geology*, *15*(5), 466–469.

Vrolijk, P. (1990), On the mechanical role of smectite in subduction zones, *Geology*, *18*(8), 703–707.

Vrolijk, P., and S. M. F. Sheppard (1991), Syntectonic carbonate veins from the Barbados accretionary prism (ODP Leg 110): Record of paleohydrology, *Sedimentology*, *38*, 671–690.

Vrolijk, P., G. Myers, and J. C. Moore (1988), Warm fluid migration along tectonic melanges in the Kodiak accretionary complex, Alaska, *J. Geophys. Res.*, *93*, 10,313–10,324.

Wang, K., R. Wells, S. Mazzotti, R. D. Hyndman, and T. Sagiya (2003), A revised dislocation model of interseismic deformation of the Cascadia subduction zone, *J. Geophys. Res.*, *108*, 2026, doi:10.1029/2001JB001227.

Wang, K. H., R. D. Yamano, and M. Makoto (1995), Thermal regime of the southwest Japan subduction zone, *Tectonophysics*, *248*, 53–69.

Witschard, M., and J. F. Dolan (1990), Contrasting structural styles in siliciclastic and carbonate rocks of an offscraped sequence: The Peralta accretionary prism, Hispaniola, *Geol. Soc. Am. Bull.*, *102*, 792–806.